



**Influence of Hydrophobic Residue on the Binding of CB[7]  
Toward Diammonium ions of Common  
Ammonium●●●Ammonium Distance**

Journal:	<i>Organic &amp; Biomolecular Chemistry</i>
Manuscript ID:	OB-ART-04-2015-000784.R1
Article Type:	Paper
Date Submitted by the Author:	23-Apr-2015
Complete List of Authors:	<p>Cao, Liping; Key Laboratory of Pesticide and Chemical Biology, Ministry of Education, Central China Normal University,, Škalamera, Đani; Rudjer Boskovic Institute, Department of Organic Chemistry and Biochemistry</p> <p>Zavalij, Peter; University of Maryland, Department of Chemistry and Biochemistry</p> <p>Hostas, Jiri; Academy of Sciences of the Czech Republic, Institute of Organic Chemistry and Biochemistry</p> <p>Hobza, Pavel; Academy of Sciences of the Czech Republic, Institute of Organic Chemistry and Biochemistry</p> <p>Mlinarić-Majerski, Kata; Ruđer Bošković Institute, Department of Organic Chemistry and Biochemistry</p> <p>Glaser, Robert; Ben Gurion University, Chemistry</p> <p>Isaacs, Lyle; University of Maryland, Department of Chemistry and Biochemistry</p>

## ARTICLE

# Influence of Hydrophobic Residues on the Binding of CB[7] Toward Diammonium ions of Common Ammonium•••Ammonium Distance

Cite this: DOI: 10.1039/x0xx00000x

Received 00th January 2012,  
Accepted 00th January 2012

DOI: 10.1039/x0xx00000x

www.rsc.org/

Liping Cao,<sup>a</sup> Đani Škalamera,<sup>b</sup> Peter Y. Zavalij,<sup>a</sup> Jiří Hostaš,<sup>c</sup> Pavel Hobza,<sup>c,d\*</sup>  
Kata Mlinarić-Majerski,<sup>b,\*</sup> Robert Glaser,<sup>c,\*</sup> Lyle Isaacs<sup>a,\*</sup>

We report the binding constants of CB[7] toward a series of naphthalene diammonium and 4,4'-dipiperidinium derivatives and compare the results with those obtained previously for CB[7]•**3b** by <sup>1</sup>H NMR and X-ray crystallography. The nature of binding in the host•guest complexes was investigated using quantum mechanical tools.

## Introduction

The cucurbit[n]uril (CB[n], n = 5, 6, 7, 8, 10) family<sup>1</sup> of molecular container compounds (Figure 1) is prepared by the condensation of glycoluril and formaldehyde under hot aqueous acidic conditions.<sup>2</sup> CB[n] compounds feature a hydrophobic cavity that is guarded by two electrostatically negative symmetry equivalent ureidyl carbonyl portals.<sup>1a,3</sup> In their pioneering work, Mock and Shih established that CB[6] is a potent receptor for alkanediammonium ions in aqueous formic acid solution.<sup>4</sup> For example, CB[6] binds selectively to hexane- and pentanediammonium ions ( $K_a \approx 10^6 \text{ M}^{-1}$ )<sup>4</sup> in preference to longer or shorter alkanediammonium ions. In 2005, Isaacs and co-workers discovered that CB[7] exhibits extreme affinity ( $K_a > 10^{12} \text{ M}^{-1}$ ) toward cationic adamantane and ferrocene derivatives (**1** and **2**) in 50 mM NaOAc buffered D<sub>2</sub>O at pH 4.74.<sup>5</sup> In 2006, we prepared diamantane diammonium ion (**3a**) but were disappointed by its modest affinity toward CB[7] ( $K_a = 1.3 \times 10^{11} \text{ M}^{-1}$ ) and therefore only reported its recognition properties toward bis-ns-CB[10] at that time.<sup>6</sup> In 2007, a team comprising the Kaifer, Isaacs, Gilson, Kim and Inoue groups reported that CB[7] binds **4** with  $K_a = 3 \times 10^{15} \text{ M}^{-1}$  in unbuffered water.<sup>7</sup> The ferrocene and bicyclooctane scaffolds were further explored by Inoue and by Kaifer.<sup>8</sup> Subsequently, a collaboration between Scherman, Nau, and DeSimone demonstrated the high energy nature of the 7-8 H<sub>2</sub>O molecules encapsulated within uncomplexed CB[7]. The release of these high energy water molecules upon formation of the CB[7]•guest complexes provides a potent enthalpic driving force even in the absence of ion-dipole interactions.<sup>1c,9</sup> Last year, we introduced diamantane derivative **3b** as the tightest binding CB[7]•guest complex known to date with  $K_a = 7.2 \times 10^{17} \text{ M}^{-1}$  in unbuffered water and  $2.1 \times 10^{15} \text{ M}^{-1}$  in 50 mM NaO<sub>2</sub>CCD<sub>3</sub> buffered D<sub>2</sub>O at pD 4.74.<sup>10</sup> From the X-ray crystal structure of CB[7]•**3b** we surmised that the reasons for the

ultratight binding include complementarity between the van der Waals surface contours of CB[7] and **3b**, the N<sup>+</sup>•••N<sup>+</sup> spacing of 7.78 Å which results in 14 optimal ion-dipole interactions, the co-linearity of the N<sup>+</sup>-N<sup>+</sup> line of the guest with the C<sub>7</sub>-axis of CB[7], and finally the hydrophobicity of the diamantane skeleton.<sup>10</sup> In order to further distinguish between the factors described above, we sought to design and study new rigid bis-quaternary ammonium compounds that feature similar N<sup>+</sup>•••N<sup>+</sup> distances but different hydrophobic scaffolds. Herein, we use competitors **5** and **6** to measure the  $K_a$  values of CB[7] toward naphthalene 7–12<sup>11</sup> and dipiperidine **13–14** derivatives along with X-ray crystallography and computational chemistry to understand the interactions in CB[7] complexes of **3b**, **9**, and **14**.

## Results and discussion

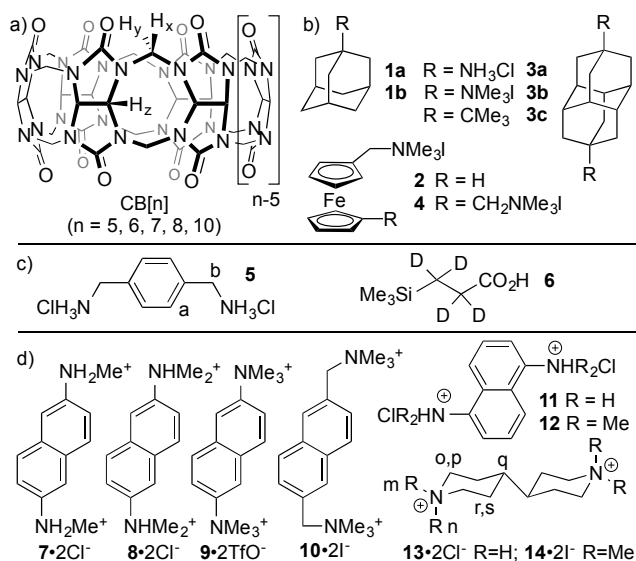


**Figure 1.** Chemical structures of: a) CB[n], b) previously studied high affinity guests for CB[7], c) competitor guests used in  $^1\text{H}$  NMR competition assays, and d) new guests studied in this paper.

The 2,6-disubstituted naphthalene (e.g. **9**) and 4,4'-dipiperidine (e.g. **14**) scaffolds are attractive candidates to hold the quaternary ammonium ions at distances similar to the 7.78 Å observed for CB[7]•**3b**. Geometry optimization of CB[7] complexes of **1b**, **3b**, **9**, and **14** were performed at the DFT-D level (BLYP-D/def2-SVP/COSMO method double-zeta + polarization, empirical dispersion, COSMO implicit solvent).<sup>12</sup> Superimposition of all non-proton atoms of the X-ray crystallographic CB[7]•**3b** structure upon corresponding atoms in the geometry optimized model afforded an RMS difference of only 0.102 Å. The  $\text{N}^+\cdots\text{N}^+$  distances in the geometry optimized models of CB[7]•**9** and CB[7]•**14** were 8.065 and 7.510 Å, respectively. Guests **9** and **14** differ from **3b** in their respective  $sp^2$ - and  $sp^3$ -hybridized carbon skeletons and their non-optimum space filling cross-sectional arrangement inside CB[7] compared with cylindrical **3b**.

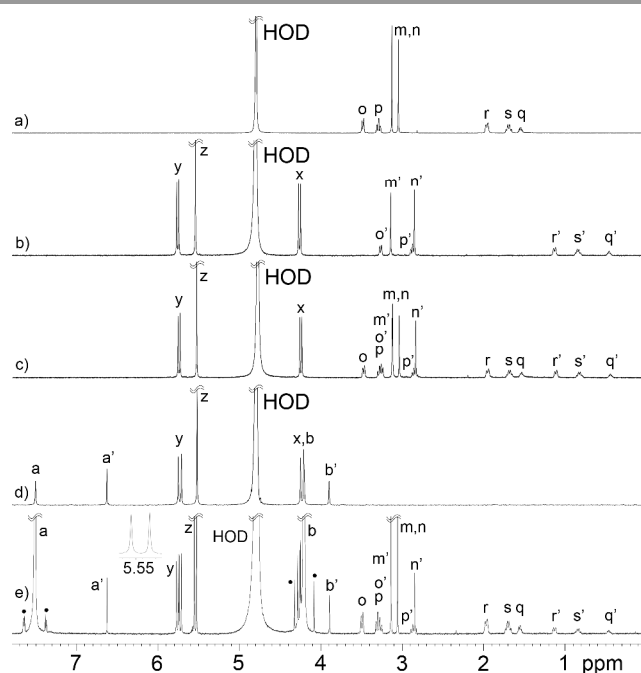


**Figure 2.** Partial  $^1\text{H}$  NMR spectra (400 MHz,  $\text{D}_2\text{O}$ , RT): a) **14** (0.25 mM); b) CB[7]•**14** (0.25 mM); c) CB[7]•**14** (0.25 mM) and **14** (0.25 mM); d) CB[7]•PXDA (0.25 mM) and **5** (0.25 mM); e) a mixture of CB[7] (0.2543 mM), **14** (0.3590 mM), and **5** (24.93 mM). Primed labels refer to CB[7]•guest complexes whereas unprimed labels refer to uncomplexed guest. • =  $^{13}\text{C}$  satellites.

In addition to **9** and **14**, we elected to study **10**, non-quaternary ammoniums **7**, **8**, and **13** as well as isomeric 1,5-naphthalene derivatives **11–12**. The binding properties of **7–14** toward CB[7] were investigated by  $^1\text{H}$  NMR spectroscopy. We found that all eight CB[7]•guest complexes (recorded at a 1:1 CB[7]•guest ratio) displayed upfield  $^1\text{H}$  NMR shifts for the central hydrophobic moiety indicative of cavity inclusion complexation as expected (Supporting Information). Guests **7–10** and **13–14** displayed slow exchange kinetics on the NMR timescale based upon the data recorded at 1:2 CB[7]•guest

ratios (Supporting Information). For example, the  $^1\text{H}$  NMR (cf. Figure 2a-c) recorded for **14**, CB[7]•**14**, and CB[7]•**14** with excess **14** illustrates slow guest exchange on the NMR timescale commonly observed for CB[7]•guest complexes.

$^1\text{H}$  NMR competition experiments were then used to measure the binding constants of CB[7] toward **7–14**.<sup>4,5,10,13</sup> To do this, an excess of two guests – one of known  $K_a$  and one of unknown  $K_a$  – compete for a limiting quantity of CB[7] (Equation 1). The concentration of the weaker binding guest is increased until the concentrations of the two competing CB[7]•guest complexes are nearly equal. Relative concentrations of the two competing complexes measured by the integrals of characteristic  $^1\text{H}$  NMR resonances for each species, combined with the known total concentrations of CB[7] and of the two competing guests, plus the mass balance expressions then allow calculation of  $K_{rel}$  and  $K_a$  according to equations 1 and 2. Figure 2c-e illustrates the  $K_a$  determination for the CB[7]•**14** complex. Competitor **5** (known  $K_a = 1.8 \times 10^9 \text{ M}^{-1}$ ) was chosen since it displays slow kinetics of exchange and sharp  $^1\text{H}$  NMR resonances (Figure 2d). Figure 2e shows the  $^1\text{H}$  NMR spectrum of a mixture of a limiting quantity of CB[7], **14** (0.3590 mM), and a large excess of the much weaker binding **5** (24.93 mM).<sup>5</sup> We use the integrals of the distinct resonances for  $\text{H}_z$  of CB[7]•**5** and CB[7]•**14** complexes at 5.56 and 5.33 ppm to determine their relative concentrations. We then used equations 1 and 2 to calculate  $K_a = (1.9 \pm 0.4) \times 10^{11} \text{ M}^{-1}$  for the CB[7]•**14** complex (Table 1).



$$\frac{K_{a,G2}}{K_{a,G1}} = \frac{\frac{[\text{CB[7]}\cdot\text{G2}]}{[\text{CB[7]}][\text{G2}]}}{\frac{[\text{CB[7]}\cdot\text{G1}]}{[\text{CB[7]}][\text{G1}]}} = \frac{[\text{CB[7]}\cdot\text{G2}][\text{G1}]}{[\text{CB[7]}\cdot\text{G1}][\text{G2}]} = K_{rel} \quad (2)$$

**Table 1.** Values of  $K_a$  ( $\text{M}^{-1}$ ) measured for CB[7]•guest complexes by  $^1\text{H}$  NMR competition experiments, 50 mM NaOAc buffered  $\text{D}_2\text{O}$  at pH 4.74.

Guest	$K_a$	Competitor
<b>7</b>	$(2.6 \pm 0.5) \times 10^8$	<b>5</b>
<b>8</b>	$(2.4 \pm 0.5) \times 10^9$	<b>5</b>
<b>9</b>	$(1.7 \pm 0.4) \times 10^{11}$	<b>5</b>
<b>10</b>	$(2.6 \pm 0.5) \times 10^{10}$	<b>5</b>
<b>11</b>	$(6.2 \pm 1.0) \times 10^6$	<b>6</b>
<b>12</b>	$(6.6 \pm 1.0) \times 10^6$	<b>6</b>
<b>13</b>	$(1.4 \pm 0.2) \times 10^{10}$	<b>6</b>
<b>14</b>	$(1.9 \pm 0.4) \times 10^{11}$	<b>5</b>

The  $K_a$  values for **7–14** toward CB[7] span more than four orders of magnitude. 1,5-Disubstituted naphthalenes **11–12** are the weakest binders. The Cambridge Structural Database (CSD) gives a 6.19(4) Å  $\text{N}^+\cdots\text{N}^+$  mean distance for **11** (and a 6.21 Å distance for a  $N,N'$ -dialkyl analogue of **12**) which are quite similar to the 6.1 Å distance between the two C=O portals of CB[7]. Guests **11** and **12** are assumed to fit the *protonated ammonium binding mode*<sup>10</sup> whereby an  $\text{NH}$  proton tilts towards the CB[7] portal rim to engender appropriate H-bonding

distances and to maximize ion-dipole interactions. These CB[7] complexes exhibit energetically costly ellipsoidal distortions which may explain their relatively low  $K_a$  values. In contrast, 2,6-disubstituted naphthalenes **7–9** feature an  $^+N\cdots N^+$  spacing closer to the 7.78 Å spacing of **3b** and an increasing number of  $N-CH_3$  groups. Interestingly,  $K_a$  for quaternary ammonium complex CB[7]•**9** is 653-fold larger than for CB[7]•**7** and 79-fold larger than for CB[7]•**8**. This can be understood by the tilting of secondary (**7**) and tertiary (**8**) diammonium ions away from the  $C_7$ -axis of CB[7] to maximize ion-dipole and H-bonding interactions. Compound **10** (with  $CH_2$  linking groups on the same 2,6-disubstituted naphthalene ring) binds 6.5-fold weaker than **9** and reinforces our *quaternary ammonium binding mode*<sup>10</sup> hypothesis that alignment of the  $C-NMe_3$  bond along the  $C_7$  symmetry axis of CB[7] is important for highest affinity. Dipiperidine compounds **13–14** have 7.26(4) Å and 7.35(8) Å  $N^+\cdots N^+$  mean distances in the CSD. Secondary ammonium dipiperidine **13** binds to CB[7] 13.6-fold weaker than quaternary ammonium **14**.

Figure 3 shows the X-ray crystal structures of CB[7]•**3b**, CB[7]•**9**, and CB[7]•**14** and an BLYP-D/def2-SVP model of [CB[7]•**1b**]<sup>+</sup>. The crystal structure of CB[7]•**9** and CB[7]•**14** exhibit two independent molecules in the asymmetric unit; the  $N^+\cdots N^+$  distances for **3b**, **9**, and **14** are 7.78, 7.94(1), and 7.39(2) Å, respectively. The longer distances for CB[7]•**3b** and CB[7]•**9** enable the  $N^+$ -atoms to respectively reside 0.799(2) and 0.91(2) Å, above each C=O portal plane. A common feature of all three crystal structures is that the  $N^+\cdots N^+$  line passes through the centroid of the equatorial plane of CB[7]. While the  $NMe_3$  units in CB[7]•**3b** exhibit approximate  $C_3$ -symmetry, those in CB[7]•**9** and CB[7]•**14** contain *diastereotopic*  $N$ -methyl groups since their  $C_{skeleton}-N^+$  bonds are not molecular rotation axes. The disparate *axial/equatorial*  $N$ -methyl dispositions in CB[7]•**14**, together with the shorter overall length of the guest, gives rise to dramatically unequal  $^+N_{methyl}-H^+\cdots O=C$  interactions. This is manifested by the centroid of **14** floating 0.8(2) Å above that of the CB[7] equatorial plane; in contrast, both **3b** and **9** are concentric with their hosts. A similar vertical mismatch (0.524 Å) is also noted in the DFT-D optimized geometry of [CB[7]•**14**]<sup>+</sup>.

The dimensions of the three hosts•guest complexes are statistically equal, e.g. 6.14(4) Å  $d(\text{centroid}_{\text{portal1}}\cdots\text{centroid}_{\text{portal2}})$ , 4.30(5) Å  $d(O\cdots\text{centroid}_{\text{portal}})$ , and 5.85(5) Å  $d(C_{\text{methine}}\cdots\text{centroid}_{\text{equator}})$ . The  $S(C_7)$  distortion index of the seven portal O-atom arrangement from ideal  $C_7$ -symmetry provides a very sensitive measure of the circularity/ellipticity of the portals.<sup>14</sup> The Avnir distance geometry  $S(C_n)$  distortion algorithm is the normalized RMS distance function from the closet theoretical  $C_n$ -symmetry construct. Its range is from 0-100, and an ideal  $C_7$ -symmetry portal oxygen arrangement affords  $S(C_7) = \text{integer zero}$ . Very low  $S(C_7)$  mean values of 0.026(7) were found for the CB[7]•**3b** diastereotopic portals compared to larger 1.0(7) mean  $S(C_7)$  measurements for less ordered seven O-atoms within each of the six portals of three empty CB[7] complexes. The

38-fold smaller  $S(C_7)$  value for CB[7]•**3b** may signify an *induced fit*. Values up to 0.1 correspond to small deviations from the ideal which may or may not be visibly perceivable.<sup>15</sup> Markedly different 0.06(4), 0.363(8)  $S(C_7)$  values of diastereotopic portals-1,2, in either mol-A or mol-B CB[7]•**9**, signify a 6-fold higher distortion of one face over the other. The two asymmetric unit molecules of CB[7]•**14** show different amounts of distortion from 7-fold ideality: 0.12(3)  $S(C_7)$  value for mol-A portals versus a 0.267(2)  $S(C_7)$  value for those of mol-B.

The smaller  $S(C_7)$  values for both portals of CB[7]•**3b** (compared to CB[7]•**9** and CB[7]•**14**) are consequences of a tighter fit between CB[7] and guest **3b** and the presence of numerous close contacts between electrostatically positive H-atoms of **3b** and the C=O portals. CB[7]•**3b** shows 7  $<2.7$  Å close contacts between  $N^+CH_3\cdots O=C$  and 11 involving  $C_{\text{Diam}}H_2\cdots O=C$ . However, there are only 7 between  $N^+CH_3\cdots O=C$  and 4  $Ar-H\cdots O=C$  close contacts in CB[7]•**9** versus 5 between  $N^+CH_3\cdots O=C$  and 7 between  $N^+CH_2\cdots O=C$  groups in CB[7]•**14**. Accordingly, we believe that the additional direct short  $H\cdots O=C$  contacts in CB[7]•**3b** relative those in CB[7]•**9** and CB[7]•**14** (Supporting Information) is an important factor governing the remarkably tight CB[7]•**3b** complex.

Although direct host-guest interactions are clearly important to the remarkable binding affinity between CB[7] and **3b**, we believe that solvation effects are also important in the binding process. The solvation of uncomplexed CB[7] consists of internal high energy waters<sup>1c,9a</sup> and external solvating water molecules. The high-energy waters influence the binding free energy differences in cases where guests of different sizes bind to hosts containing varying cavities (such as CB[n] for  $n = 6-8$ ). However, when comparing a set of similarly sized guests that displace all of the high energy waters in the cavity of a single CB[n] host, as is the case in this study, the differential effect of the high-energy water on the binding free energy is negligible.

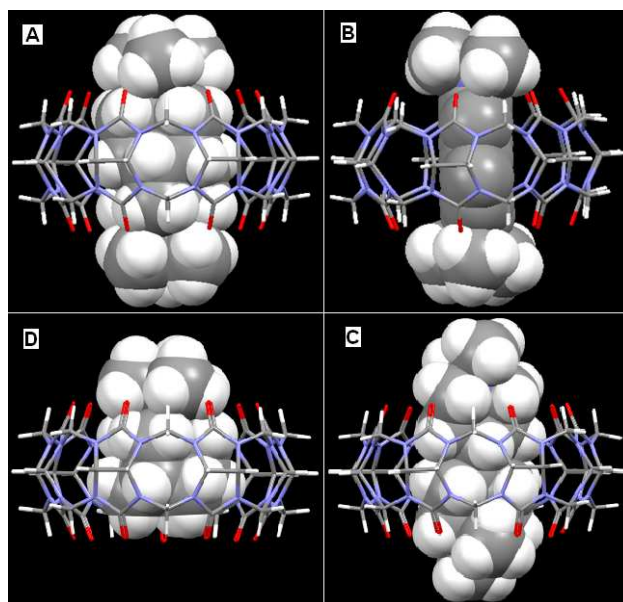


**Figure 3.** X-ray crystal structures of: A) CB[7]•**3b**, B) CB[7]•**9**, and C) CB[7]•**14**. D) BLYP-D/def2-SVP model of CB[7]•**1b**. Color code: C, grey; H, white; N, blue; O, red.

Interaction energies in a water continuum ( $IE_{\text{cosmo}}$ ) were calculated for optimized complexes using the BLYP-D3/def2-TZVPP/COSMO technique (triple-zeta + polarization, empirical dispersion, COSMO implicit solvent). Interaction energies (IE) encompass electrostatic, polarization, charge-transfer, dispersion and exchange-repulsion energies and were calculated in-vacuo ( $IE_{\text{vacuo}}$ ). When calculated in implicit solvent,  $IE_{\text{COSMO}}$ , it includes the change of solvation energy ( $\Delta SE$ ) *i.e.*  $SE_{\text{complex}} - (SE_{\text{host}} + SE_{\text{guest}}) = IE_{\text{cosmo}} - IE_{\text{vacuo}}$ .  $\Delta G_{\text{calcd}} = [(IE_{\text{COSMO}}) + \text{entropy}(T\Delta S) + \text{deformation energy} (\text{Def}_{\text{Guest}}) + \text{Def}_{\text{Host}}]$ , see values in Table 2. Dispersion energy in the computational models were calculated separately, and thus it is possible to evaluate the role of dispersion to the binding (Table 3). Other terms are included in DFT energy and cannot be separated. The most important among them is electrostatic energy and it is approximated using the Coulomb law that considers the atomic partial charges determined at the BLYP/def2-SVP level. Electrostatic energy ( $E_{\text{es}}$ ) =  $[E_{\text{es,complex}} - (E_{\text{es,host}} + E_{\text{es,guest}})]$ , cf. Table 3. Table 2 shows that the loss of entropy upon binding, calculated at the molecular mechanics level rigid-rotor-harmonic-oscillator approximation, is approximately the same for all complexes. Furthermore, deformation energies ( $\text{Def}_{\text{host}}$ ) and ( $\text{Def}_{\text{guest}}$ ) were small as expected.  $IE_{\text{vacuo}}$  are dramatically reduced in a water continuum ( $IE_{\text{cosmo}}$ ).  $IE_{\text{cosmo}}$  and  $IE_{\text{vacuo}}$  do not correlate, which reflects the important role of  $H_2O$  on the binding process. The largest  $\Delta G_{\text{calcd}}$  was found for CB[7]•**3b** and is in accord with  $\Delta G_{\text{Exptl}}$ . The remaining three  $\Delta G_{\text{Exptl}}$  values are similar and are roughly in agreement with the  $\Delta G_{\text{calcd}}$  values.

A satisfactory  $\rho^2 = 0.8$  correlation between  $\Delta G_{\text{calcd}}$  and  $\Delta G_{\text{Exptl}}$  values was found when a larger set of 10 host•guest complexes was considered (Supplementary Information). We can thus conclude that the advanced theoretical model used in the present study describes the nature of binding reasonably well in the complexes studied. The main trends of these calculations will be presented below. As expected, **3b** and its *t*-Bu isostere **3c** fill the CB[7] cavity more efficiently than **9** or **14** which is reflected in the 33% larger dispersion energies calculated for CB[7]•**3b** and CB[7]•**3c** than for CB[7]•**9** or CB[7]•**14** (Table 3). The markedly decreased values of electrostatic and  $\Delta SE$  for CB[7]•**3c** relative to CB[7]•**3b** dramatically emphasize the importance of the  $^+NMe_3$  groups in the binding process. Notably, the auspicious 7.8(3) Å  $Me_2\text{-}_3N^+\cdots^+NMe_2\text{-}_3$  spacing of **3b**, **9**, and **14** afforded comparably large values of  $E_{\text{es}}$  (−177(1) kcal/mol) for their CB[7] complexes. Finally, the less favorable solvation ( $SE_{\text{guest}}$ ) of the more hydrophobic guest **3b** relative to **9** and **14** as well as the less unfavorable change in solvation ( $\Delta SE$ ) for CB[7]•**3b** compared to CB[7]•**9** and CB[7]•**14** play a role in the observed ultratight affinity of the CB[7]•**3b** complex.

**Table 2.** Values of  $IE_{\text{vacuo}}$ ,  $IE_{\text{COSMO}}$ ,  $\Delta S$ ,  $\text{Def}_{\text{Guest}}$ ,  $\text{Def}_{\text{Host}}$ ,  $\Delta G_{\text{calcd}}$  and  $\Delta G_{\text{Exptl}}$  calculated for CB[7]•guest model complexes (kcal/mol).

CB[7]•Guest	$IE_{\text{vacuo}}$	$IE_{\text{COSMO}}$	TAS	$\text{Def}_{\text{Guest}}$	$\text{Def}_{\text{Host}}$	$\Delta G_{\text{calcd}}$	$\Delta G_{\text{Exptl}}$
CB[7]• <b>3b</b> <sup>+2</sup>	−147.6	−47.3	4.5	0.5	1.05	−41.3	−20.50
CB[7]• <b>9</b> <sup>+2</sup>	−144.6	−35.7	3.9	0.3	1.70	−29.8	−15.1
CB[7]• <b>14</b> <sup>+2</sup>	−139.4	−31.8	5.1	0.4	1.54	−24.8	−15.1
CB[7]• <b>1b</b> <sup>+1</sup>	−84.9	−33.9	3.3	0.2	0.40	−30.0	−16.4
CB[7]• <b>3c</b>	−45.2	−28.3	3.3	0.5	3.70	−20.8	-

**Table 3.** Values of Dispersion Energy, Electrostatic Energy ( $E_{\text{es}}$ ),  $\Delta$ Solvation Energy ( $\Delta SE$ ) and  $SE_{\text{guest}}$  calculated (298K) for CB[7]•guest model complexes (kcal/mol).  $SE_{\text{CB[7]host}} = -108$  kcal/mol.

CB[7]•Guest	Dispersion	$E_{\text{es}}$	$\Delta SE$	$SE_{\text{guest}}$	$SE_{\text{complex}}$
CB[7]• <b>3b</b> <sup>+2</sup>	−72.4	−175.5	100.3	−141.3	−148.7
CB[7]• <b>9</b> <sup>+2</sup>	−47.9	−177.5	108.9	−145.0	−141.1
CB[7]• <b>14</b> <sup>+2</sup>	−48.9	−178.4	107.6	−148.0	−148.4
CB[7]• <b>1b</b> <sup>+1</sup>	−53.5	−93.4	51.0	−47.3	−104.0
CB[7]• <b>3c</b>	−68.9	−1.9	16.9		

## Conclusions

In summary, the  $K_a$  values of CB[7] toward 1,5- and 2,6-disubstituted naphthalenes **7–12** and 4,4'-dipiperidines **13–14** were determined. Quaternary ammonium guests **9**, **10**, and **14** gave the largest  $K_a$  values because they are vertically disposed within CB[7]. Secondary and tertiary ammonium compounds tilt away from the pseudo  $C_7$ -axis of CB[7] to form  $^+NH\cdots Q=C$  H-bonds resulting in energetically costly CB[7] cage distortions. The remarkably similar  $N^+\cdots N^+$  distances for **3b** and **9** in their CB[7] crystal structures allowed us to further refine our understanding of the factors governing high affinity binding. The multiple  $CH_{\text{guest}}\cdots Q=C_{\text{host}}$  close contacts, the collinearity of the  $N^+\cdots N^+$  line and  $C_7$ -axis of CB[7], and the critical  $N^+\cdots N^+$  distance of 7.78 Å are particularly important non-covalent interactions favoring the high affinity binding of **3b** for CB[7]. The work deepens our understanding of factors governing the formation of CB[n]•guest complexes and more broadly of non-covalent forces governing high affinity interactions in  $H_2O$  that are relevant to a variety of biomolecular recognition events.

## Experimental

**General Experimental.** Starting materials were purchased from commercial suppliers and were used without further purification or were prepared by literature procedures. Melting points were measured on a Meltemp apparatus in open capillary tubes and are uncorrected. IR spectra were measured on a JASCO FT/IR 4100 spectrometer and are reported in  $cm^{-1}$ . NMR spectra were measured on commercial spectrometers operating at 600 MHz and 400 MHz for  $^1H$  and 125 MHz for  $^{13}C$ . Mass spectrometry was performed using a JEOL AccuTOF electrospray instrument (ESI).

**Compound 14.** A mixture of 4,4'-bipiperidine (200 mg, 1.20 mmol), MeI (3.4 g, 24 mmol) and NaHCO<sub>3</sub> (222 mg, 2.6 mmol) was dissolved in MeOH (25 mL) and the mixture was stirred and refluxed for 48 h. The mixture then was cooled to room temperature, and was centrifuged at 7200 rpm for 5 min. The supernatant was decanted and the precipitate was washed with Et<sub>2</sub>O (30 mL), and centrifuged at 7200 rpm for 5 min. The precipitate was dried under high vacuum to give **14** as white powder (535 mg, 1.11 mmol, 93%). M.p. >300 °C. IR (KBr, cm<sup>-1</sup>): 3040w, 3004m, 2961s, 2924m, 2861m, 1473s, 1463s, 1406m, 1286m, 1210m, 1034m, 959m, 949m, 918s. <sup>1</sup>H NMR (600 MHz, D<sub>2</sub>O): 3.48 (d, *J* = 13.9, 4H), 3.29 (t, *J* = 11.8, 4H), 3.13 (s, 6H), 3.05 (s, 6H), 1.96 (d, *J* = 13.9, 4H), 1.75-1.65 (m, 4H), 1.60-1.50 (m, 2H). <sup>13</sup>C NMR (125 MHz, D<sub>2</sub>O, dioxane as internal reference): 62.5, 56.1, 47.0, 36.3, 23.4. HR-MS: *m/z* 353.1437 ([14-I]<sup>+</sup>, calcd. for C<sub>14</sub>H<sub>30</sub>N<sub>2</sub>I<sup>+</sup>, 353.1454).

### Acknowledgements

We thank the United States National Science Foundation (CHE-1404911 to L.I.), Croatian Ministry of Science, Education and Sports (grant 098-0982933-2911 to K. M.-M.), Ben-Gurion Univ. Scientific Relations Research Fund (R. G.), Institute of Organic Chemistry and Biochemistry of the Academy of Science of the Czech Republic (RVO: 61388963 to P. H.), and the Czech Science Foundation (P208/12/G016 to P. H.) for financial support. We thank Dr. Avital Steinberg for the S(C<sub>7</sub>) calculations.

### Notes and references

<sup>a</sup>Department of Chemistry and Biochemistry, University of Maryland, College Park, MD 20742; <sup>b</sup>Department of Organic Chemistry and Biochemistry, Ruder Bošković Institute, Bijenička cesta 54, 10000 Zagreb, Croatia; <sup>c</sup>Institute of Organic Chemistry and Biochemistry, Academy of Sciences of the Czech Republic, 16610 Praha 6, Czech Republic; <sup>d</sup>Regional Center of Advanced Technologies and Materials, Department of Physical Chemistry, Palacký University, 771 46 Olomouc, Czech Republic; <sup>e</sup>Department of Chemistry, Ben-Gurion University of the Negev, Beer-Sheva 84105, Israel.

\*Please address correspondence to Pavel Hobza (pavel.hobza@uochb.cas.cz), Kata Mlinarić-Majerski (majerski@irb.hr), Robert Glaser (rglaser@bgu.ac.il), or Lyle Isaacs (lisaacs@umd.edu).

† Details of <sup>1</sup>H NMR competition experiments, X-ray crystallographic results (CB[7]•**9**, CCDC 1057202; CB[7]•**14**, CCDC 1057201), coordinates of geometry optimized models. See DOI: 10.1039/b000000x/

- 1) (a) J. W. Lee, S. Samal, N. Selvapalam, H.-J. Kim and K. Kim *Acc. Chem. Res.* 2003, **36**, 621-630; (b) J. Lagona, P. Mukhopadhyay, S. Chakrabarti and L. Isaacs *Angew. Chem., Int. Ed.* 2005, **44**, 4844-4870; (c) W. M. Nau, M. Florea and K. I. Assaf *Isr. J. Chem.* 2011, **51**, 559-577; (d) E. Masson, X. Ling, R. Joseph, L. Kyeremeh-Mensah and X. Lu *RSC Adv.* 2012, **2**, 1213-1247.
- 2) (a) W. A. Freeman, W. L. Mock and N.-Y. Shih *J. Am. Chem. Soc.* 1981, **103**, 7367-7368; (b) J. Kim, I.-S. Jung, S.-Y. Kim, E. Lee, J.-K. Kang, S. Sakamoto, K. Yamaguchi and K. Kim *J. Am. Chem. Soc.* 2000, **122**, 540-541; (c) A. Day, A. P. Arnold, R. J. Blanch and B. Snushall *J. Org. Chem.* 2001, **66**, 8094-8100; (d) A. I. Day, R. J. Blanch, A. P. Arnold, S. Lorenzo, G. R. Lewis and I. Dance *Angew. Chem., Int. Ed.* 2002, **41**, 275-277; (e) S. Liu, P. Y. Zavalij and L. Isaacs *J. Am. Chem. Soc.* 2005, **127**, 16798-16799.
- 3) W. Ong and A. E. Kaifer *Organometallics* 2003, **22**, 4181-4183.

- 4) W. L. Mock and N.-Y. Shih *J. Org. Chem.* 1986, **51**, 4440-4446.
- 5) S. Liu, C. Ruspic, P. Mukhopadhyay, S. Chakrabarti, P. Y. Zavalij and L. Isaacs *J. Am. Chem. Soc.* 2005, **127**, 15959-15967.
- 6) W.-H. Huang, S. Liu, P. Y. Zavalij and L. Isaacs *J. Am. Chem. Soc.* 2006, **128**, 14744-14745.
- 7) M. V. Rekharsky, T. Mori, C. Yang, Y. H. Ko, N. Selvapalam, H. Kim, D. Sobransingh, A. E. Kaifer, S. Liu, L. Isaacs, W. Chen, S. Moghaddam, M. K. Gilson, K. Kim and Y. Inoue *Proc. Natl. Acad. Sci. U. S. A.* 2007, **104**, 20737-20742.
- 8) (a) S. Moghaddam, C. Yang, M. Rekharsky, Y. H. Ko, K. Kim, Y. Inoue and M. K. Gilson *J. Am. Chem. Soc.* 2011, **133**, 3570-3581; (b) A. E. Kaifer, W. Li and S. Yi *Isr. J. Chem.* 2011, **51**, 496-505.
- 9) (a) F. Biedermann, V. D. Uzunova, O. A. Scherman, W. M. Nau and A. De Simone *J. Am. Chem. Soc.* 2012, **134**, 15318-15323; (b) F. Biedermann, W. M. Nau and H.-J. Schneider *Angew. Chem., Int. Ed.* 2014, **53**, 11158-11171.
- 10) L. Cao, M. Sekutor, P. Y. Zavalij, K. Mlinarić-Majerski, R. Glaser and L. Isaacs *Angew. Chem., Int. Ed.* 2014, **53**, 988-993.
- 11) D. Škalamera, L. Cao, L. Isaacs, R. Glaser and K. Mlinarić-Majerski 2015, unpublished results.
- 12) (a) S. Grimme, J. Antony, Ehrlich, S. and H. Krieg *J. Chem. Phys.* 2010, **132**, 154104; (b) TURBOMOLE v6.5 2013, a development of University of Karlsruhe and Forschungszentrum Karlsruhe GmbH, 1898-2007, TURBOMOLE GmbH, since 2007; available from <http://www.turbomole.com>.
- 13) L. Cao and L. Isaacs *Supramol. Chem.* 2014, **26**, 251-258.
- 14) (a) H. Zabrodsky, S. Peleg and D. Avnir *J. Am. Chem. Soc.* 1992, **114**, 7843-7851; (b) H. Zabrodsky, S. Peleg and D. Avnir *J. Am. Chem. Soc.* 1993, **115**, 8278-8289.
- 15) R. Glaser *Symmetry, spectroscopy, and crystallography: The structural nexus*; Wiley-VCH: Weinheim, 2015,